Meningioma 1 is indispensable for mixed lineage leukemia-rearranged acute myeloid leukemia

Amit Sharma,[1] Nidhi Jyotsana,[1] Razif Gabdoulline,[1] Dirk Heckl,[2] Florian Kuchenbauer,[3] Robert K. Slany,[4] Arnold Ganser[1] and Michael Heuser[1]

[1]Department of Hematology, Hemostasis, Oncology and Stem Cell Transplantation, Hannover Medical School, Hannover, Germany; [2]Department of Pediatric Hematology and Oncology, Hannover Medical School, Hannover, Germany; [3]British Columbia Cancer Agency, Vancouver, British Columbia, Canada and [4]Department of Genetics, Friedrich-Alexander-University Erlangen-Nürnberg, Erlangen, Germany

 doi:10.3324/haematol.2018.211201

Received: November 6, 2018.

Accepted: August 8, 2019.

Pre-published: August 14, 2019.

Correspondence: *MICHAEL HEUSER* - heuser.michael@mh-hannover.de

MN1 is indispensable for MLL-rearranged acute myeloid leukemia

Supplementary Information

Supplementary Materials and Methods

Viral vectors vector production, and CRISPR

Retroviral vector MSCV- MLL-AF9-IRES-GFP was received as a gift from Dr. Florian Kuchenbauer, University Hospital Ulm, Germany. MN1 expression was restored using the MSCV-MN1-IRES-YFP plasmid as described previously (1). Lentiviral particles were produced by transient transfection of 293T cells using CaCl2 method. Briefly, constructs were co-transfected with CRISPR vector, pMD2.G and pSPAX2 and viral supernatant was collected after 48-72hr which was further concentrated 100x by ultracentrifugation. Viral supernatants were used to transduce murine or human leukemic cell lines in the presence of 5 µg/mL protamine sulfate (Sigma-Aldrich, Seelze, Germany). Transduced cells (CRISPR dTomato+) were single cell sorted in 96 well plates using the FACSAria Fusion sorter (Becton Dickinson, Heidelberg, Germany) and cultured in medium conditions as described below. Clones derived from single cells were further used for sequencing and *in vitro/in vivo* experiments. For all human cell line MN1-CRISPR experiments, sgRNA-2 (sg-2) was used except for Supplementary Figure S3 where we used sgRNA-4 (sg-4). The list of sgRNAs is summarized in Supplementary Table S1.

Cell lines and primary cells

MLL-AF9 murine leukemic cells were prepared from primary mouse bone marrow cells as described above. Cells were sorted for GFP and maintained in Dulbecco's modified Eagle's medium (DMEM) (STEM cell Technologies, Cologne, Germany) supplemented with 15% fetal bovine serum (PAA, Cölbe Germany), 10 ng/mL of human interleukin-6 (hIL-6), 6 ng/mL of murine interleukin-3 (mIL-3), and 20 ng/mL of murine stem cell factor (mSCF) (all from Peprotech, Hamburg, Germany)(1, 2). Human cell lines (THP-1, MV-4-11, NB4, U937, K562, Kasumi-1, HL-60, ME-1 and HEL) were maintained in RPMI medium (Thermo Fisher Scientific, Darmstadt, Germany) supplemented with 10 or 20%

fetal bovine serum (as recommended by DSMZ, Braunschweig, Germany). Human cell lines OCI-AML2 and OCI-AML3 (DSMZ, Braunschweig, Germany) were maintained in MEM alpha medium (Thermofisher) supplemented with 20% fetal bovine serum. CD34+ healthy bone marrow cells and AML patient's cells were cultured in IMDM medium (12440, Life Technologies) with 10% FCS (Hyclone, Logan, UT), 1% Peniciliin/Streptomycin (PAA laboratories, Pasching, Austria), 200 mM L-Glutamine (Thermo Fisher Scientific), 0.01 M ß-mercaptoethanol (Sigma-Aldrich) 20 ng/ml each of human IL3, human IL6, human GM-CSF, human G-CSF and human SCF (Peprotech).

Apoptosis, differentiation and cell cycle analysis

For apoptosis measurements, $1x10^5$ cells were stained with Annexin V-APC according to the manufacturer`s protocol (BD Pharmingen Cat no. 550474) and analyzed on a BD FACS ARIA flow cytometer (Becton Dickinson, Heidelberg, Germany). Differentiation analysis of murine cell lines was performed using flow cytometry as previously described (1). For immunophenotyping, monoclonal antibodies used were Allophycocyanin- (APC) labelled c-kit (2B8) from BD Biosciences and CD11b-APC (M 1/70) from eBiosciences. Cell cycle analysis was performed by *in vitro* labelling with 10 µM of BrdU, which was added to 0.5 $x10^6$ cells for 6 hours. Cell cycle analysis was performed according to the manufacturer's protocol (BD Pharmingen Cat no. 557892) All the FACS analysis for apoptosis, differentiation and cell cycle experiments were performed on BD LSRII cytometer.

Mouse transplantation and homing assay

For subcutaneous transplantation, 6-8 weeks old NOD-SCID female mice were injected subcutaneously with THP-1 and MV-4-11 (MN1 wild type (wt) or MN1null clones) ($2x10^6$ cells dissolved in matrigel, BD Biosciences) in the left and right flanks. Tumor volume was monitored using a Vernier caliper at regular time intervals as mentioned in the graph. For intravenous transplantation, human cells were injected into the tail vein of 6-8 weeks old female NSG mice (previously irradiated with 2.5 Gy). For intravenous transplantation in C57BL6/J mice, murine cells were injected into the tail vein of 6-8 weeks old female

C57BL6/J mice (previously irradiated with 8 Gy), together with a life-sparing dose of 1 x 10^5 freshly isolated bone marrow cells from syngeneic mice.

Transplanted cells were monitored by cheek or retro-orbital vein bleeds and FACS analysis of GFP and or dTomato expressing cells every four weeks by immunophenotypic analysis using the BD LSRII flow cytometer (Becton Dickinson). Blood counts with differential WBC analysis were performed using an ABC Vet Automated Blood counter (Scil animal care company GmbH, Viernheim, Germany). At death, peripheral blood, bone marrow and spleen samples were analyzed for GFP/dTomato/CD45-APC (human) positive cells and differentiation markers as described previously (1). Cytospin preparations from bone marrow and spleen were stained with Wright-Giemsa stain. OlympusXC50 (Olympus) and analySIS software (Soft Imaging System, Stuttgart, Germany) were used to capture images.

For the homing assay, MLL-AF9/Mn1wt and MLL-AF9/Mn1null cells ($1*10^6$ cells/mouse) (GFP and dTomato positive CRISPR clone) were injected into the tail vein of irradiated (8 Gy total-body irradiation). Mice were sacrificed at 8 and 24 hours post transplantation and harvested bone marrow cells were analyzed by flow cytometry.

Immunoblotting

Cell lysates were prepared with lysis buffer (20 mM HEPES, pH 7.5, 0.4 M NaCl; 1 mM EDTA, 1 mM EGTA, 1 mM DTT) supplemented with a protease inhibitor cocktail tablet (Roche Diagnostics, Mannheim, Germany). Extracted proteins were separated by sodium dodecyl sulphate-polyacrylamide gel electrophoresis (SDS-PAGE), transferred to nitrocellulose membrane (GE life sciences, Freiburg, Germany), and membranes were incubated with anti-MN1 (Abcam ab112916) and anti-ß-actin (A2228, Sigma-Aldrich, Germany) according to the manufacturer's protocol. Chemiluminescence was used for visualization using Clarity Western ECL Substrate (Bio-Rad) or SignalFire Plus ECL Reagent (Cell Signaling Technology, Germany) with a ChemiDoc MP Imaging System (Bio-Rad, Munich, Germany).

DNA/RNA isolation and quantitative reverse-transcriptase polymerase chain reaction (RT-PCR)

Genomic DNA was extracted using the QIAmp DNA Mini or Micro Kit (Qiagen, Hilden, Germany) according to the manufacturer's protocols. Total RNA was purified from cells with the RNeasy Micro or Mini Kit (Qiagen). cDNA was synthesized using the cDNA Reverse Transcription Kit (Thermo Fisher Scientific), according to the manufacturer's instructions.

Quantitative RT-PCR was performed as previously described using SYBR green (Qiagen) on a StepOnePlus Real-Time PCR system (Thermo Fisher Scientific)(5). Relative expression was determined with the $2^{-\Delta\Delta CT}$ method, and the house keeping gene transcript *Abl1 or ABL1 or GAPDH (as mentioned)* was used to normalize the results. The primers are listed in Supplementary Table S1.

siRNA and Lipidnanoparticles (LNPs)

Briefly, our lipid mixture contained a proprietary lipid mix (SUB9KIT, Precision Nanosystems, Vancouver, Canada, with minor modifications). DiI-C18 from Life Technologies (D-282) was added to prepare fluorescently labelled LNPs to further monitor their uptake in cells. DiI has an excitation wavelength of 549 nm and emission wavelength of 565 nm. LNPs were packaged with siRNA using a microfluidic system for controlled mixing conditions on the NanoAssemblr™ instrument (Precision Nanosystems). LNP-siRNA formulations were formed by injecting the lipid/ethanol solution into the first inlet, and a low pH aqueous buffer (sodium acetate buffer 25mM, pH 4) containing siRNA in the second inlet of the microfluidic chip. The microfluidic mixing took place at a flow rate of 12ml/min, with siRNA to lipid flow ratio of 3:1. The formed LNP-siRNA formulation further underwent dialysis, filtration and quantification before use. The list of siRNAs is summarized in Supplementary Table S1.

Clonogenic progenitor assay

CD34+ bone marrow cells from healthy donors and AML patient's cells were cultured overnight in suspension medium as mentioned above with control or anti-MN1 siRNA

packaged in LNPs (5, 6). Methocult H4100 medium (Stem Cell Technologies Inc., Vancouver, Canada) was used and supplemented with 10 ng/mL human IL3, 10 ng/mL human GM-CSF, 50 ng/mL human SCF, 50 ng/mL human FLT3 ligand and 3 U/mL human EPO (all from Peprotech). For CD34+ healthy and AML patient's cells, $1.5x10^5$ human mononuclear cells were plated in duplicate with control or anti-MN1 siRNA packaged in LNPs at a dose of 4µg/ml. Colony-forming cells (CFCs) from murine cell lines were assayed as previously described (1, 5). One thousand GFP+ dTomato+ cells per dish were plated in duplicate. Both human and murine colonies were evaluated microscopically between 7 to 14 days after plating by standard criteria. Colony pictures were taken at 100-fold magnification using an Olympus CX41 microscope (Olympus, Tokyo, Japan) and Olympus camera C5060 (Olympus, Tokyo, Japan).

Gene expression and CHIP-seq analysis

Microarray data was analyzed using R packages (https://www.R-project.org/). Arrays were background corrected, normalized and summarized with the *rma* function of the *affy* package(7); the *limma* package(8) was used to select differentially expressed genes adjusting the false discovery rate using the Benjamini-Hochberg procedure. The Broad Institute GSEA software package was applied for gene set enrichment analysis using gene ontology gene sets from the Molecular Signatures Database (http://www.broad.mit.edu/gsea/msigdb/).

Chip-Seq data sets (H3K79me2 GSE55038 (9), MLL-AF9 from GSE29130 (10), Hoxa9 from GSE33518 (11), MN1 and MEIS1 (12) are freely accessible at https://www.ncbi.nlm.nih.gov/gds. These data sets have been derived from immortalized mouse bone marrow cells (by specific oncogenes Hoxa9, MN1, MEIS1 and MLL-AF9) and it is notable that our model system also uses MLL-AF9 to immortalize mouse bone marrow cells. The MACS2 program(13) was used to define the peaks of the binding regions. Histograms showing the number of peaks within 40 bp intervals were generated using Chip-Seq tools (14).

Supplementary figures:

Supplementary Figure S1.

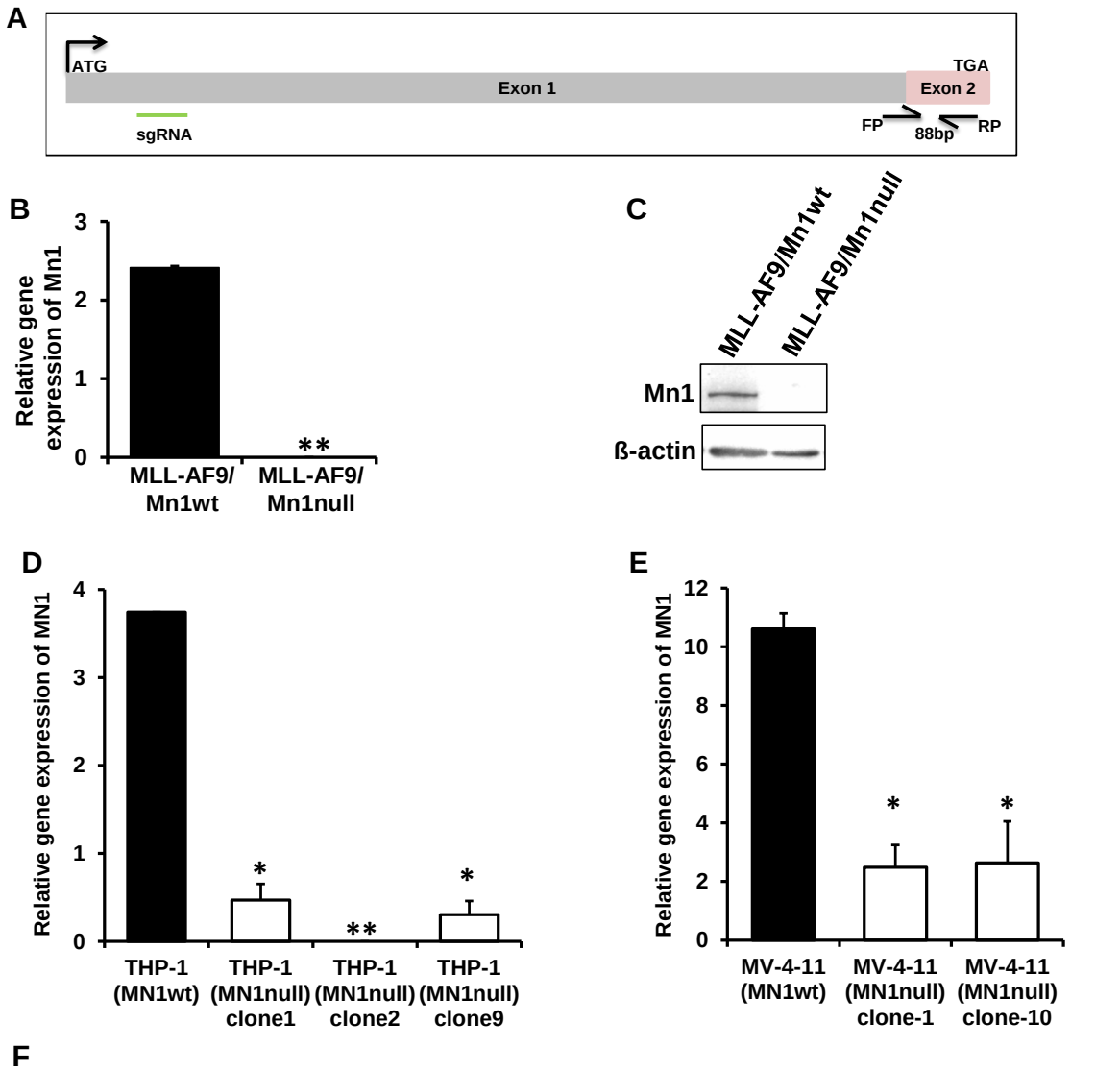

Supplementary Figure S1. Validation of CRISPR/Cas9-mediated MN1 deletion.

A. Schematic showing position of sgRNA, exons and qRT-PCR primer position on MN1 consensus coding DNA sequence.

B. Relative gene expression of *Mn1* normalized to *Abl1* in MLL-AF9/Mn1wt and MLL-AF9/Mn1null cells (mean ± SEM, n=3).

C. Representative western blot showing protein expression of Mn1 in MLL-AF9 (Mn1wt or null) cells.

D. Relative gene expression of *MN1* normalized to *GAPDH* in THP-1/MN1wt and THP-1/MN1null cells (3 clones) (mean ± SEM, n=3).

E. Relative gene expression of *MN1* normalized to *GAPDH* in MV-4-11/MN1wt and MV-4-11/MN1null cells (2 clones) (mean ± SEM, n=3).

F. Analysis of genomic MN1 breakpoints in THP-1/MV-4-11cells for different clones. The genomic MN1 breakpoints generated by the CRISPR-Cas9 system in THP-1/MV-4-11 cells were analyzed by PCR and sequenced by Sanger sequencing. Alignment of the sequences compared to the predicted MN1 breakpoint are shown as point mutations, deletions and insertions for the respective clones (for additional information, see Supplementary Table S3).

*P<0.05; **P<0.01; ns, not significant.

Supplementary Figure S2.

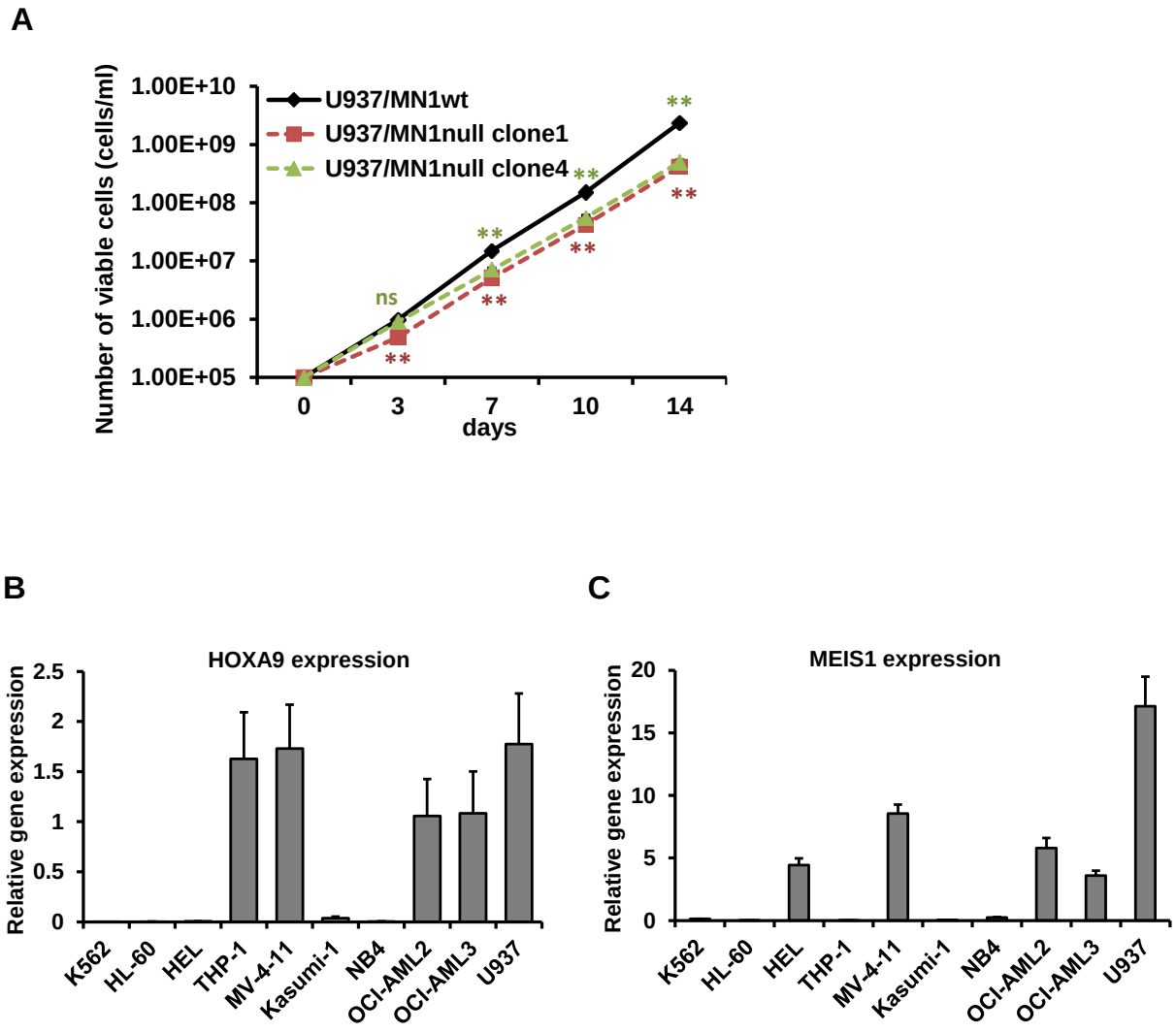

Supplementary Figure S2. Effect of MN1 deletion on proliferation in non-MLL rearranged human leukemia cell lines and gene expression of *HOXA9* and *MEIS1* in human cell lines.

A. Cumulative cell counts of U937/MN1wt and U937/MN1null cells (mean ± SD, n=3).

B-C. Relative gene expression of *HOXA9* and *MEIS1* normalized to *ABL1* in different human leukemia cell lines (mean ± SEM, n=4).

*P<0.05; **P<0.01; ns, not significant.

Supplementary Figure S3.

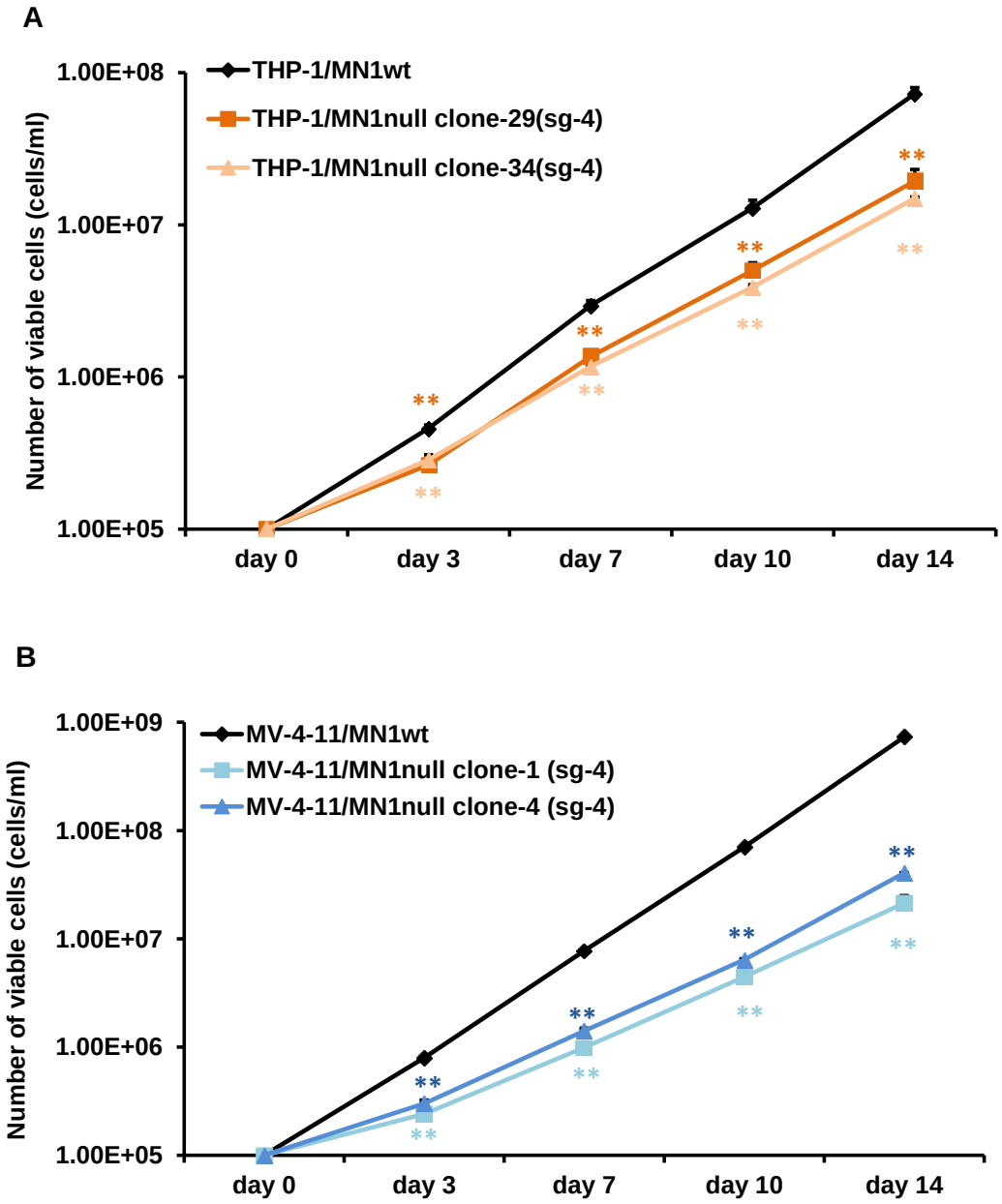

Supplementary Figure S3. Effect of MN1 deletion using a second independent sgRNA on proliferation of MLL positive cell lines.

A. Cumulative cell counts of THP-1/MN1wt and THP-1/MN1null cells (mean ± SD, n=3).

B. Cumulative cell counts of MV-4-11/MN1wt and MV-4-11/MN1null cells (mean ± SD, n=3). *P<0.05; **P<0.01; ns, not significant.

Supplementary Figure S4.

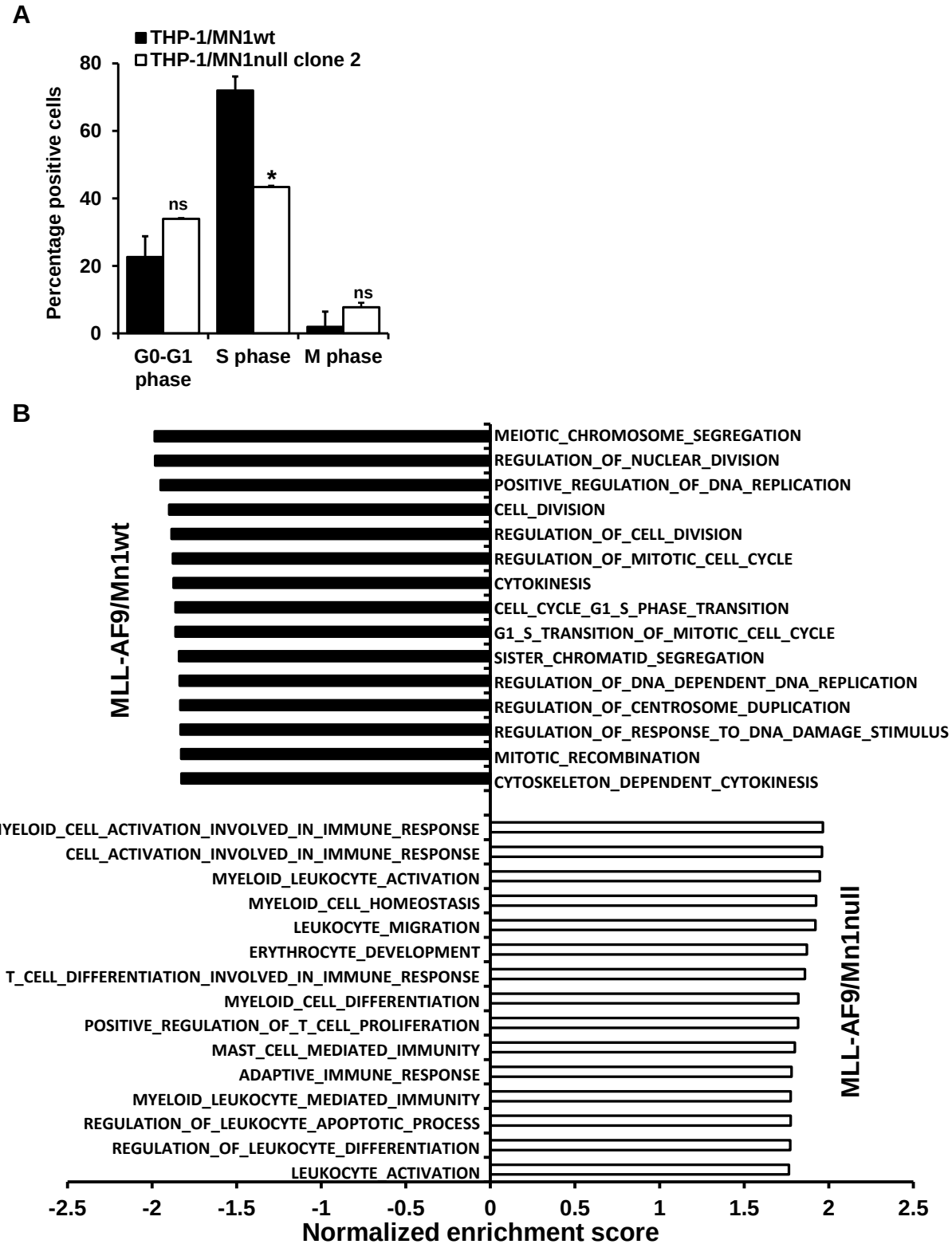

Supplementary Figure S4. MN1 regulates the cell cycle in MLL-rearranged leukemias.

A. Cell cycle analysis of THP-1 (MN1wt or MN1null) cells (mean ± SEM, n=3).

B. Relevant top 15 enriched gene ontology gene sets from gene set enrichment analysis in MLL-AF9/Mn1wt and MLL-AF9/Mn1null cells using gene expression profiling data. See also Supplementary Table S5.

*P<0.05; **P<0.01; ns, not significant.

Supplementary Figure S5.

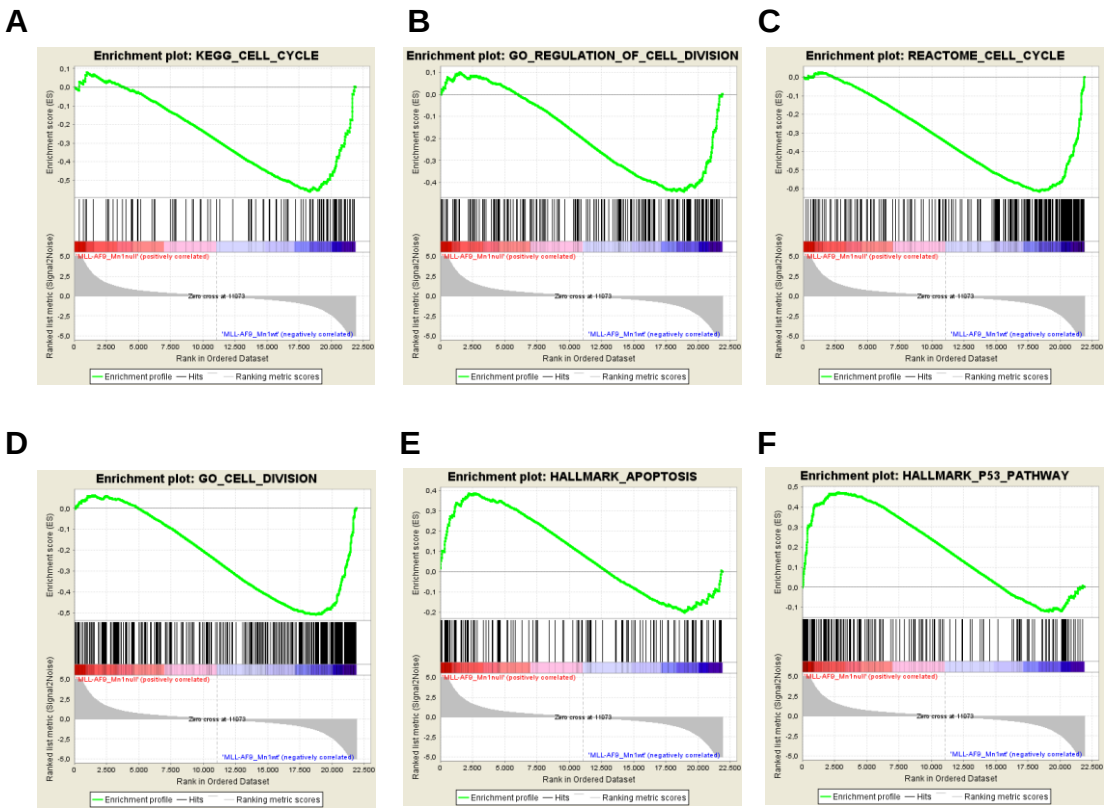

Supplementary Figure S5. MN1 regulates cell cycle and apoptosis in MLL-rearranged leukemias based on gene expression data.

A-D. Enrichment plots for the gene sets “KEGG cell cycle”, “regulation of cell division”, “reactome cell cycle”, “GO cell division” comparing MLL-AF9/Mn1wt and MLL-AF9/Mn1null cells. See also Supplementary Table S4.

E-F. Enrichment plots for the gene sets “Hallmark Apoptosis” and “Hallmark P53 pathway” comparing MLL-AF9/Mn1wt and MLL-AF9/Mn1null cells. See also Supplementary Table S4.

Supplementary Figure S6.

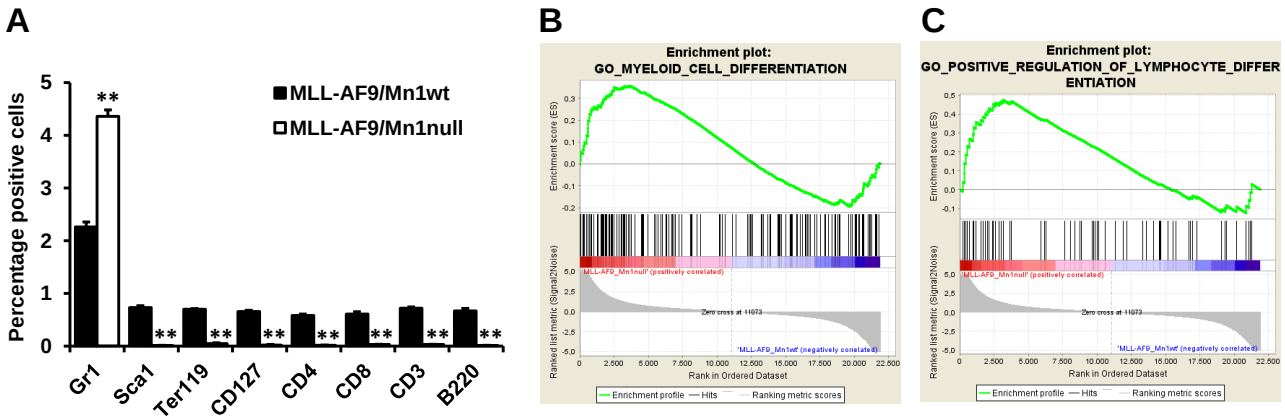

Supplementary Figure S6. MN1 regulates differentiation in MLL-rearranged leukemias based on gene expression data.

A. Immunophenotype of in vitro cultured MLL-AF9/Mn1wt and MLL-AF9/Mn1null cells (mean ± SEM, n=3).

B-C. Enrichment plots for the gene sets “myeloid cell differentiation” and “positive regulation of lymphocyte differentiation” comparing MLL-AF9/Mn1wt and MLL-AF9/Mn1null cells. See also Supplementary Table S4.

*P<0.05; **P<0.01; ns, not significant.

Supplementary Figure S7.

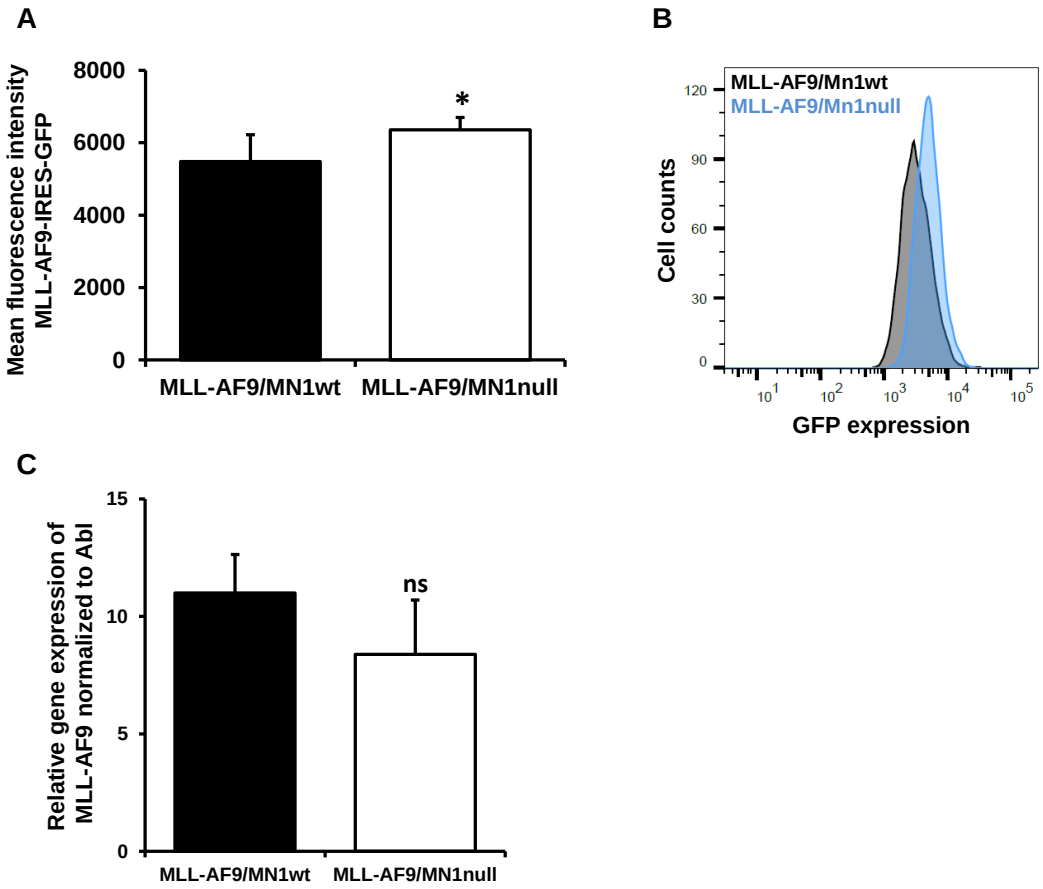

Supplementary Figure S7. MLL-AF9 expression in MLL-AF9-Mn1wt or MLL-AF9-Mn1null) cells.

A-B. Mean Fluorescence intensity (MFI) analysis (GFP) of MLL-AF9/Mn1wt and MLL-AF9/Mn1null cells (mean ± SEM, n=3) and FACS plot showing mean fluorescent intensity (MFI) analysis (GFP) of MLL-AF9/Mn1wt and MLL-AF9/Mn1null cells.

C. Relative gene expression of *MLL-AF9* normalized to *Abl1* in MLL-AF9/Mn1wt and MLL-AF9/Mn1null cells (mean ± SEM, n=3). *P<0.05; **P<0.01; ns, not significant.

Supplementary Figure S8.

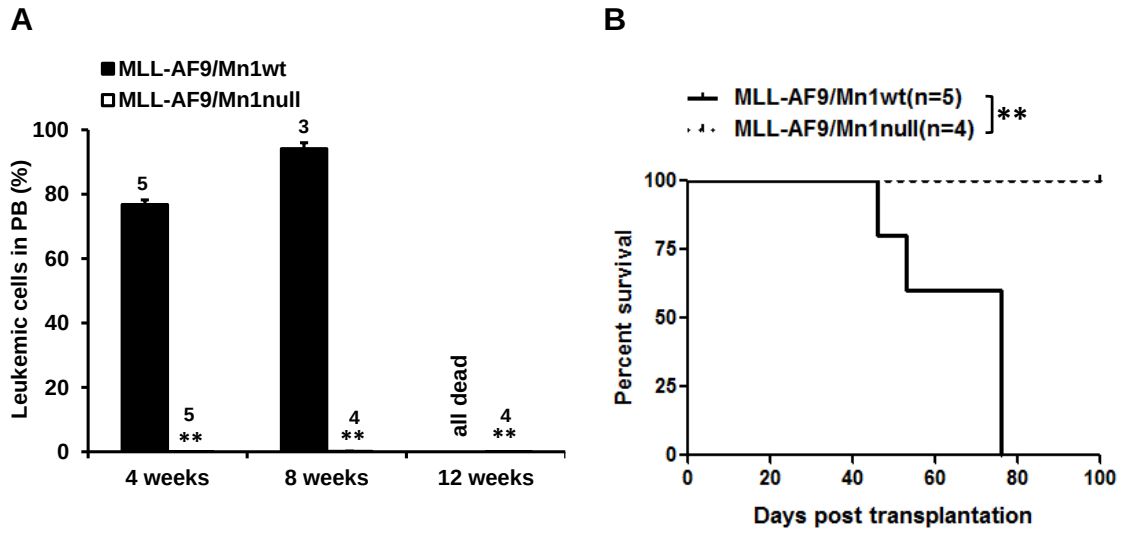

Supplementary Figure S8. Transplantation of MLL-AF9/Mn1wt or MLL-AF9/Mn1null cells in NSG mice.

A. Engraftment of MLL-AF9/Mn1wt and MLL-AF9/Mn1null cells in peripheral blood (PB) of NSG mice at 4, 8 and 12 weeks after transplantation (mean ± SEM of the indicated number of mice).

B. Survival of mice receiving transplants of MLL-AF9/Mn1wt and MLL-AF9/Mn1null cells (log-rank test) (n=5 for MLL-AF9/Mn1wt and n=4 for MLL-AF9/Mn1null). *P<0.05; **P<0.01; ns, not significant.

Supplementary Figure S9.

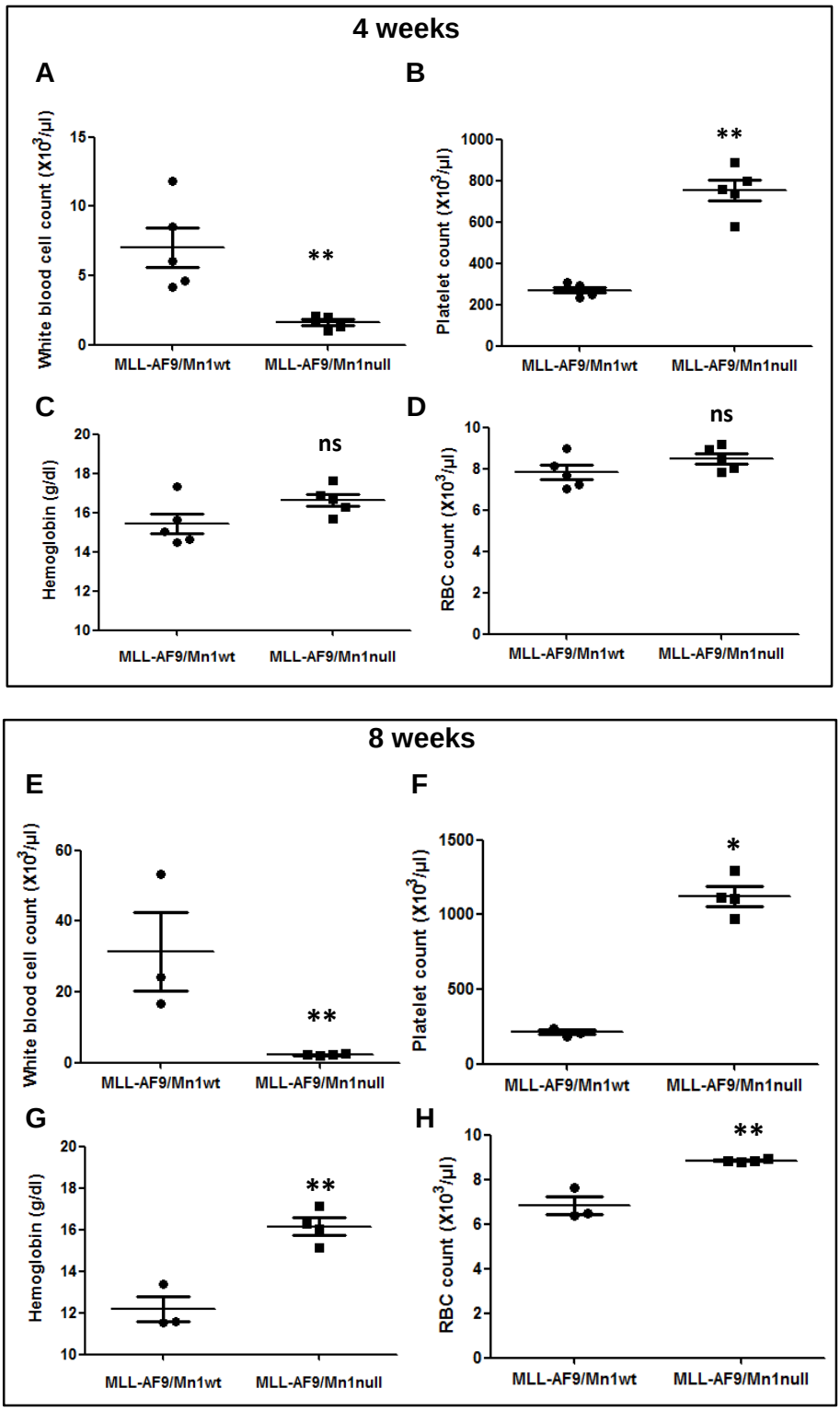

Supplementary Figure S9. Blood counts at 4 and 8 weeks in mice receiving MLL-AF9/Mn1wt or MLL-AF9/Mn1null cells in NSG mice.

A-H. Blood counts (WBC, platelets, hemoglobin and RBC) in peripheral blood of mice at 4 and 8 weeks. Mice received transplants of MLL-AF9/Mn1wt and MLL-AF9/Mn1null cells (mean ± SEM); (at 4 weeks: n=5 for MLL-AF9/Mn1wt and n=4 for MLL-AF9/Mn1null; at 8 weeks: n=3 for MLL-AF9/Mn1wt and n=4 for MLL-AF9/Mn1null).

*P<0.05; **P<0.01; ns, not significant.

Supplementary Figure S10.

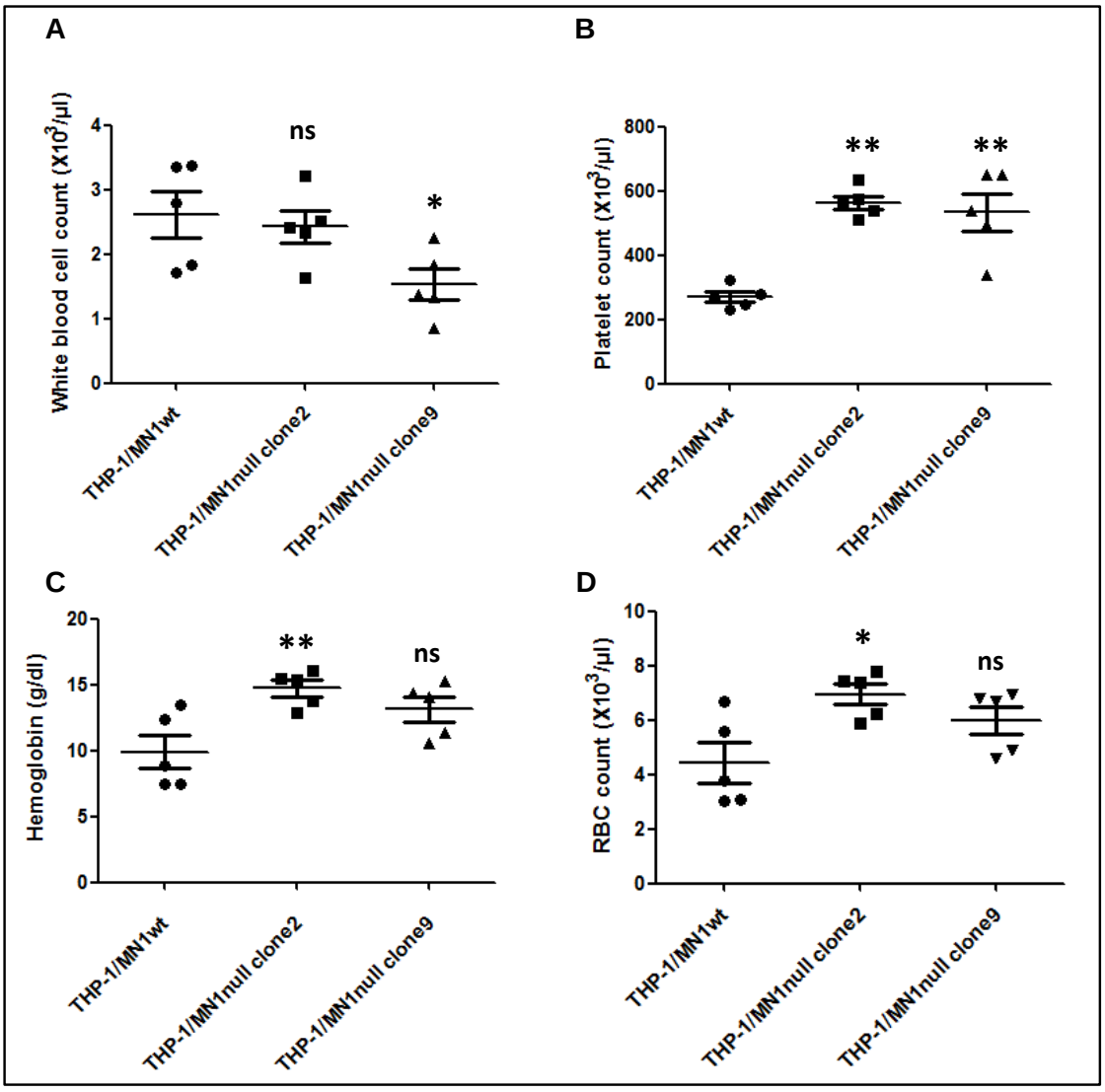

Supplementary Figure S10. Blood counts at 4 weeks in mice receiving transplants of THP-1/MN1wt or THP-1/MN1null cells injected intravenously in NSG mice.

A-D. Blood counts (WBC, platelets, hemoglobin and RBC) in peripheral blood of mice at 4 weeks. Mice received transplants of THP-1/MN1wt and THP-1/MN1null cells by intravenous injection (mean ± SEM; n=5 for THP-1/MN1wt, THP-1/MN1null clone2 and 9). *P<0.05; **P<0.01; ns, not significant.

Supplementary Figure S11.

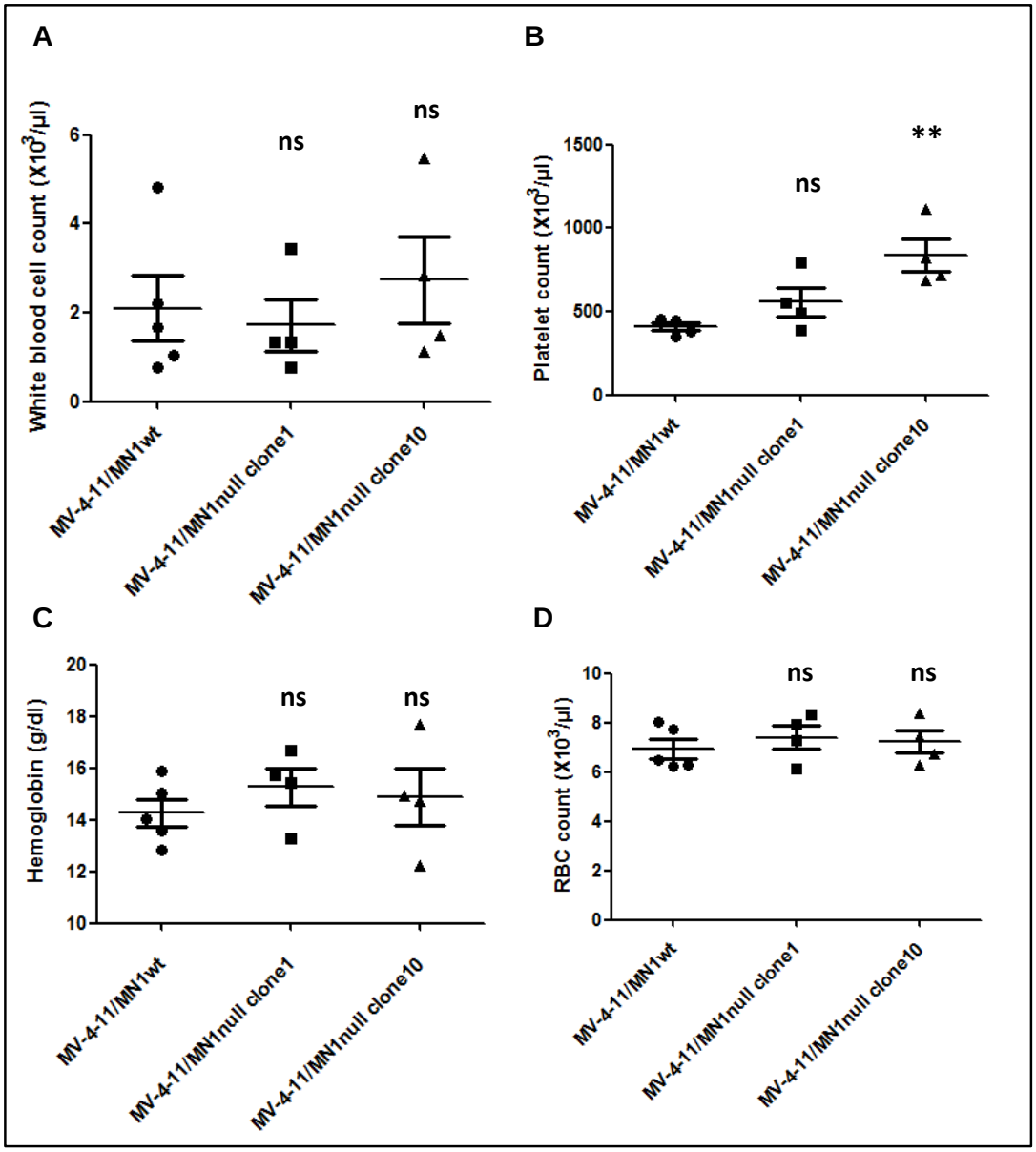

Supplementary Figure S11. Blood counts at 4 weeks in mice receiving transplants of MV-4-11/MN1wt or MV-4-11/MN1null cells injected intravenously in NSG mice.

A-D. Blood counts (WBC, platelets, hemoglobin and RBC) in peripheral blood of mice at 4 weeks. Mice received transplants of MV-4-11/MN1wt and MV-4-11/MN1null cells by intravenous injection (mean ± SEM; n=5 for MV-4-11/MN1wt, n=4 for MV-4-11/MN1null clone1 and 10). *P<0.05; **P<0.01; ns, not significant.

Supplementary Figure S12.

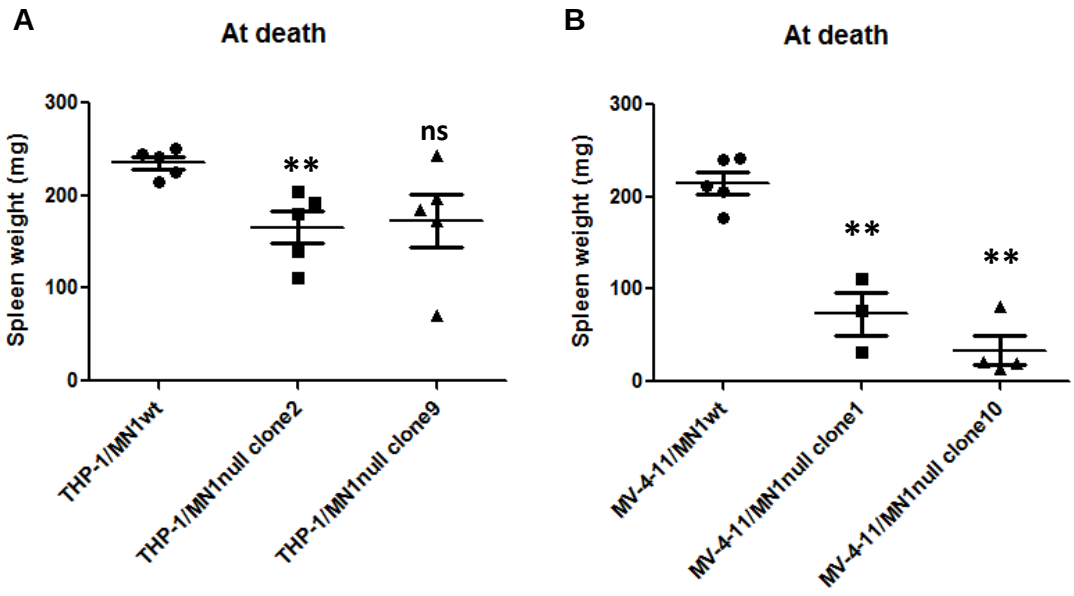

Supplementary Figure S12. Spleen weight at sacrifice in mice that received transplants of THP-1 (MN1wt or MN1null) and MV-4-11 (MN1wt or MN1null) cells injected intravenously in NSG mice.

A-B. Spleen weight at sacrifice of mice that received intravenous transplants of THP-1 and MV-4-11 (MN1wt or MN1null) cells (mean ± SEM; n=5 for THP-1/MN1wt and THP-1/MN1null clone2 and 9; n=5 for MV-4-11/MN1wt, n=3 for MV-4-11/MN1null clone1 and n=4 for MV-4-11/MN1null clone10). *P<0.05; **P<0.01; ns, not significant.

Supplementary Figure S13.

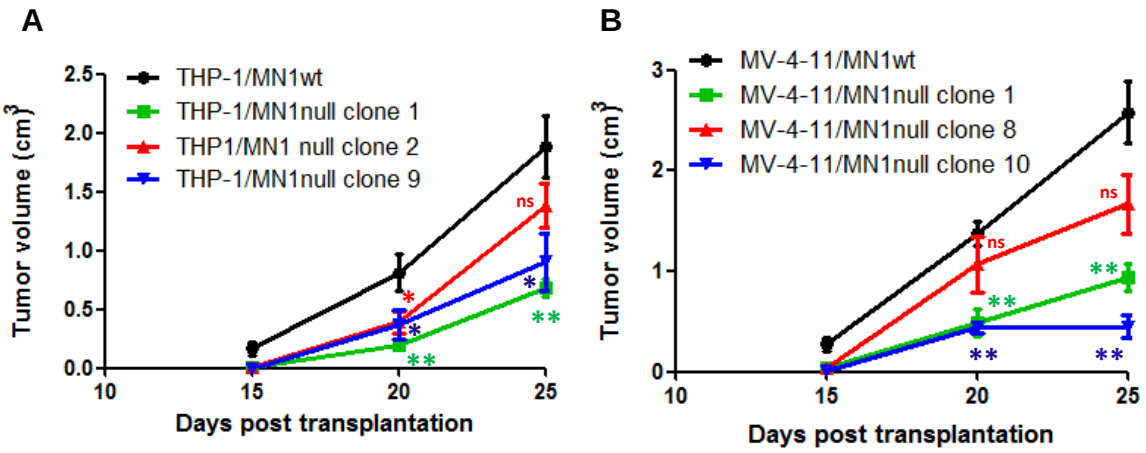

Supplementary Figure S13. Tumor volume at different time points in mice that received transplants of THP-1 and MV-4-11 cells (MN1wt or MN1null) injected subcutaneously in NOD-SCID mice.

A. Tumor volume of THP-1/MN1wt and THP-1/MN1null cell clones transplanted in NOD-SCID mice (mean ± SEM; THP-1/MN1wt, n=8; THP-1/MN1null clone 1, n=10; THP-1/MN1null clone 2, n=8; THP-1/MN1null clone 9, n=8).

B. Tumor volume of MV-4-11/MN1wt and MV-4-11/MN1null cell clones transplanted in NOD-SCID mice (mean ± SEM, MV-4-11/MN1wt, n=6; MV-4-11/MN1null clone 1, n=8; MV-4-11/MN1null clone 8, n=8; MV-4-11/MN1null clone 10, n=6).

*P<0.05; **P<0.01; ns, not significant.

Supplementary Figure S14.

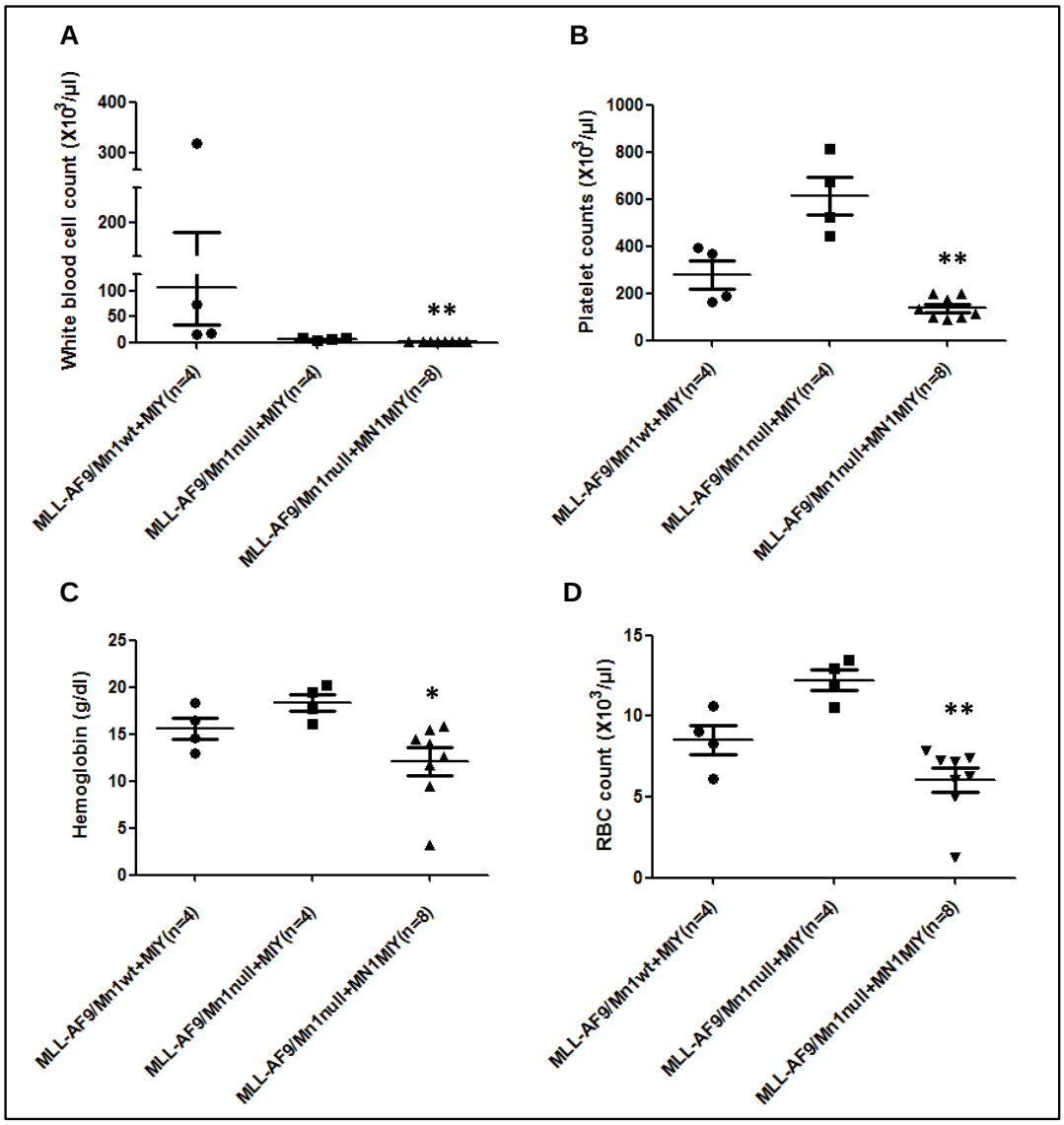

Supplementary Figure S14. MN1 overexpression restores leukemogenicity in MLL-AF9/Mn1null cells: blood counts at 4 weeks.

A-D. Blood counts (WBC, platelets, hemoglobin and RBC) in peripheral blood of mice at 4 weeks. Mice received transplants of MLL-AF9/Mn1wt and MLL-AF9/Mn1null cells transduced with control (MIY) or MN1-MIY plasmid (mean ± SEM of the indicated number of mice). *P<0.05; **P<0.01; ns, not significant.

Supplementary Figure S15.

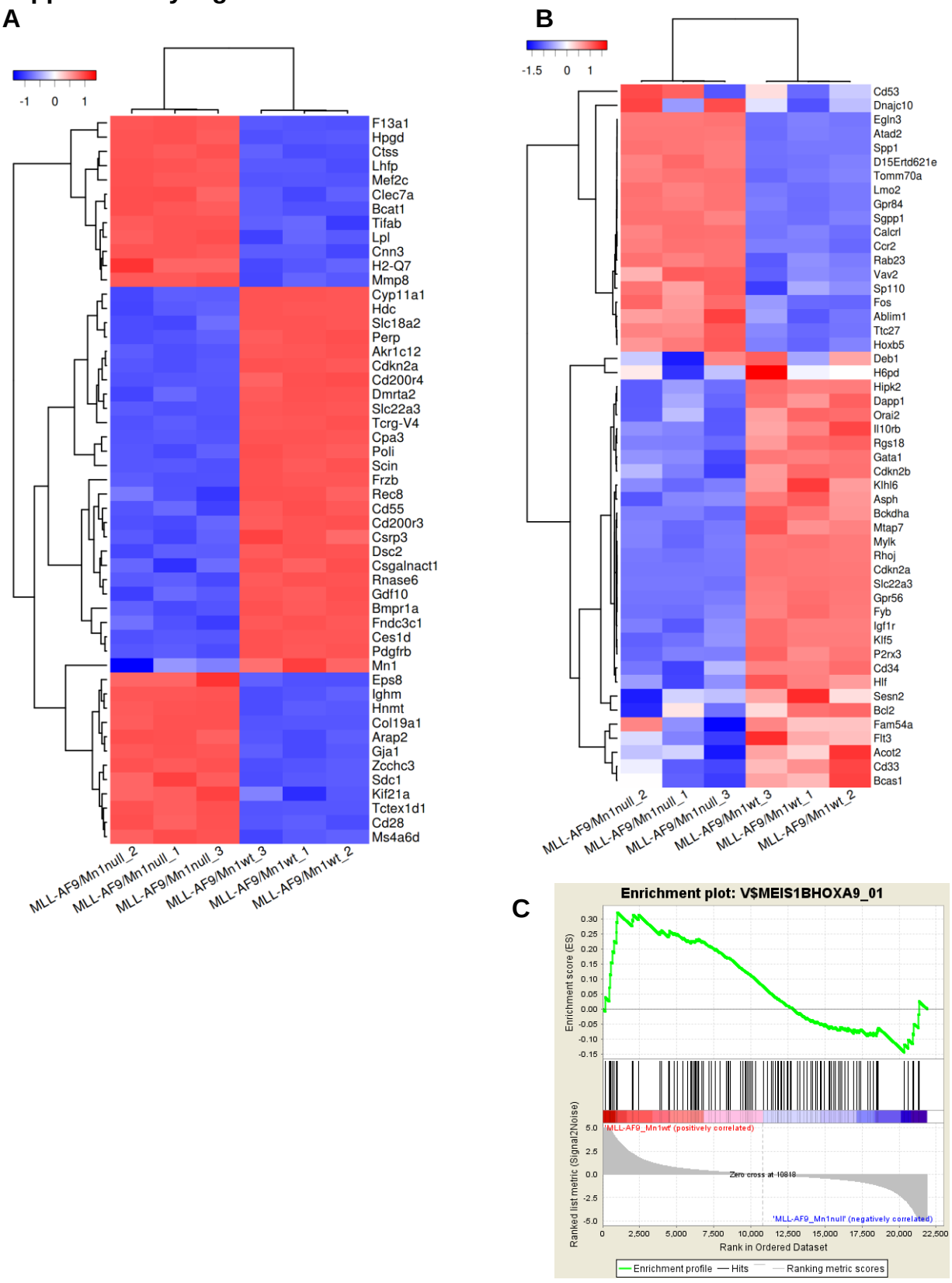

Supplementary Figure S15. Gene expression analysis of MLL-AF9/Mn1wt versus MLL-AF9/Mn1null cells.

A. Heatmap from unsupervised hierarchical clustering showing the top 50 differentially expressed genes in MLL-AF9/Mn1wt versus MLL-AF9/Mn1null cells. Expression values, gene list and fold changes are provided in Supplementary Table S6.

B. Heatmap from microarray data of the top 50 differentially expressed Hoxa9/Hoxa10 target genes between MLL-AF9/Mn1null and MLL-AF9/Mn1wt cells. Significantly more Hoxa9/Hoxa10 target genes were downregulated than upregulated in MLL-AF9/Mn1null cells compared to MLL-AF9/Mn1null cells (P=0.027 from hypergeometric distribution). The expression values, the gene list and fold changes are provided in Supplementary Table S7.

C. Enrichment plot for the gene set V$MEIS1BHOXA9_01 of the Transcription Factor Targets dataset of GSEA comparing MLL-AF9/Mn1wt and MLL-AF9/Mn1null cells. GSEA reported NES=1.218, FDR=0.229.

Supplementary Figure S16.

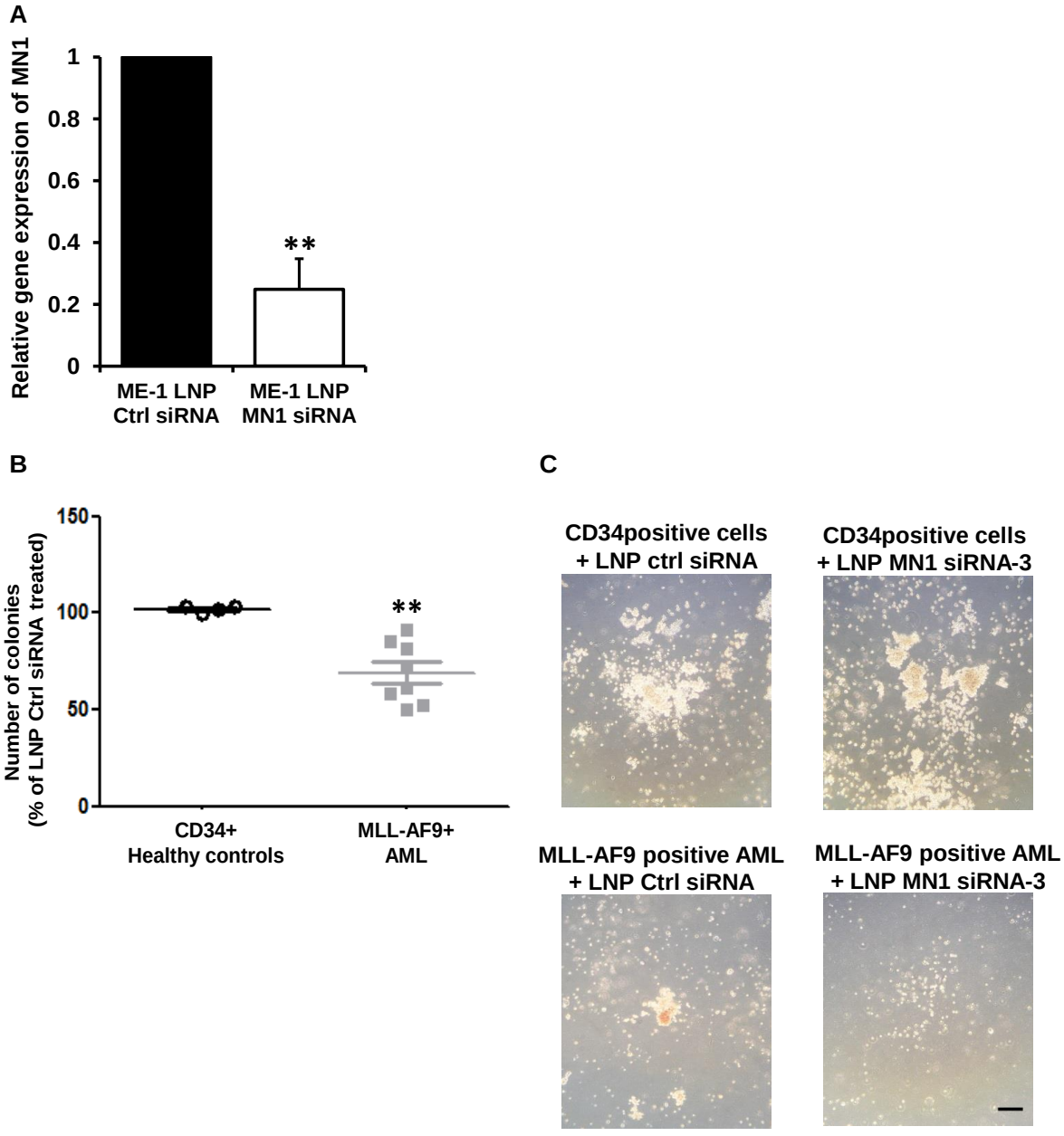

Supplementary Figure S16. LNP/siRNA-mediated knockdown of MN1 in ME-1 cells and primary human samples.

A. Relative gene expression of *MN1* normalized to *ABL1* in ME-1 cells treated with anti-MN1 or control siRNA packaged in lipid nanoparticles (mean ± SEM, n=3).

B. CFC counts of CD34+ healthy control cells and MLL-AF9 positive AML patient cells treated with anti-MN1 siRNA-3/LNP formulation normalized to cells treated with the control siRNA/LNP formulation (mean ± SEM, cells from 1 CD34+ healthy donor with 4 repeats, and cells from 4 MLL-AF9 positive AML patients in duplicate from each patient).

C. Morphology of representative CFC colonies of CD34+ healthy controls and MLL-AF9 positive AML patient cells treated with control or anti-MN1-3 siRNA/LNP formulation taken after 12 days. Black scale bar represents 0.25 mm.
*P<0.05; **P<0.01; ns, not significant.

Supplementary Table S1. Table with sequences of siRNA, qRT-PCR primers, sequencing primers and sgRNAs.

siRNA	**Sequence**
MN1 sense	5'-UCGACUCGCUGGAAUACAA-3'
MN1 antisense	5'-TTGTUTTCCUGCGUGTCGU-3'
MN1 - 3 sense	5'-CAAGAGAGCGCGUGGUUCU-3'
MN1 - 3 antisense	5'-GUUCUCUCGCGCACCAAGA-3'
Control - AHA1_sense	5'-GGAuGAAGuGGAGAuuAGudTsdT -3'
Control- AHA1_antisense	5'-ACuAAUCUCcACUUcAUCCdTsdT -3'
RT-PCR primers	**Sequence**
Abl_F	CTGGGGCTCAAAGTCAGATG
Abl_R	CTGTTTGAAGTTGGTGGGCT
Bcl2-I-1_F	GCTGGGACACTTTTGTGGAT
Bcl2-I-1_R	GTCATGCCCGTCAGGAAC
Bcl2-I-2_F	GGCGGAGTTCACAGCTCTAT
Bcl2-I-2_R	GTCCTCACTGATGCCCAGTT
Bcl2-I-11_F	CGACAGTCTCAGGAGGAACC
Bcl2-I-11_R	ATTTGCAAACACCCTCCTTG
Bcl2_F	GATAACGGAGGCTGGGATG
Bcl2_R	GCTGAGCAGGGTCTTCAGAG
Mcl1_F	GCTTCATCGAACCATTAGCA
Mcl1_R	CATCCCAGCCTCTTTGTTTG

GAPDH F	GATCATCAGCAATGCCTCCT
GAPDH R	GGACTGTGGTCATGAGTCCT
MN1_F	CAAAGAAGCCCACGACCTC
MN1_R	CGTCACCCACGTCGTCTG
Meis1_F	ATGGCGCAAAGGTACGAC
Meis1_R	GGGTCCCCATACATCGTG
Survivin_F	CAACCCGATAGAGGAGCATAG
Survivin_R	CTTGGCTCTCTGTCTGTCCA
Hoxa9_F	CCCATCGATCCCAATAACC
Hoxa9_R	CTTCTCCAGTTCCAGCGTCT
HoxA10_F	GACTCCCTGGGCAGTTCC
HoxA10_R	TGTAAGGGCAGCGTTTCTTC
HoxB4_F	CACGGTAAACCCCAATTACG
HoxB4_R	TCCTTCTCCAACTCCAGGAC
Ctnnb1_F	AGAGCAAGCTCATCATTCTGG
Ctnnb1_R	GACAGACAGCACCTTCAGCA
Mn1_F	CAAAGAAGCCCATGACCACC
Mn1_R	ATCTGTGCAGTGGACAGTCA
HOXA9_F	CCCATCGATCCCAATAACC
HOXA9_R	CAGTTCCAGGGTCTGGTGTT
MEIS1_F	CGCAAAGGTACGACGATCTA
MEIS1_R	ATGCGGGTCCCCATACAT
MLL-AF9_F	GCTTAGGGATCCTTGAAGTGAA

MLL-AF9_R	TGCCTTGTCACATTCACCAT
CRISPR_seq_primers	**Sequence**
MN1_F	ATGAACACCCACTTTAAGGC
MN1_R	GGCACCTGAACTGTGGAAGT
Mn1_F	ATGTTTGGGCTGGACCAA
Mn1_R	TGCAGACATGAGGCACCTGG
sgRNA	**Sequence**
Human MN1(sg-2) (Oligo_F)	CACCGCAGATCAACAGCCGGCACGC
Human MN1(sg-2) (Oligo_R)	AAACGCGTGCCGGCTGTTGATCTGC
Murine Mn1 (Oligo_F)	CACCGCCGCGCGCGTGGAAGCCGTA
Murine Mn1 (Oligo_R)	AAACTACGGCTTCCACGCGCGCGGC
Human MN1(sg-4) (Oligo_F)	CACC GTCGCCCAGCGCGCTCATAGC
Human MN1 (sg-4) (Oligo_R)	AAAC GCTATGAGCGCGCTGGGCGAC

Supplementary Table S2. Mn1/MN1 deletion clones in mouse/human leukemia cell lines.

Cell line	Sorted clones	Viable clones	Wildtype clones	Mutant clones	Viable /sorted %	Mutant /sorted %
Mouse bone-marrow cells						
Hoxa9	288	0	0	0	0	0
Hoxa9 Meis1	288	0	0	0	0	0
MLL-AF9	288	1	0	1	0.34	0.34
E2A-HLF	288	15	15	0	5.20	0

Human leukemia cell lines									
Cell line	Sorted clones	Viable clones	Wildtype clones	Mutant clones	Viable /sorted %	Mutant /sorted %	MLL status	HOXA9 expression	MEIS1 expression
THP-1	288	42	38	4	14.58	1.38	+	1.627	0.007
MV-4-11	192	15	4	11	7.81	5.72	+	1.729	8.548
NB4	192	11	4	0	5.7	0	-	0.005	0.253
OCI-AML2	192	58	51	7	30.20	3.64	-	1.056	5.803
OCI-AML3	192	43	43	0	22.39	0	-	1.082	3.593
U937	192	12	5	7	6.25	3.64	-	1.774	17.119
K562	192	40	23	17	12.5	8.85	-	0.036	0.133
Kasumi-1	96	12	7	5	18.75	5.20	-	0.000	0.042
HL-60	96	18	14	4	12.5	4.16	-	0.002	0.002
HEL	96	12	12	0	14.58	0	-	0.006	4.434

Supplementary Table S3. MN1 deletion clones in human leukemia cell lines.

MN1 CRISPR clone	Deletion (base pairs –bp)
U937/MN1null clone1	8 bp deletion and mismatches
U937/MN1null clone4	5 bp deletion and mismatches
THP-1/MN1null clone29 (sg-4)	10 bp deletion
THP-1/MN1null clone34 (sg-4)	55 bp del and mismatches
MV-4-11/MN1null clone1 (sg-4)	19 bp deletion and mismatches
MV-4-11/MN1null clone4 (sg-4)	19 bp deletion

Supplementary Table S4. Normalized enrichment scores and P-values for GSEA plots (see Supplementary Figure S5 and S6).

Figure	Categories	NES	p-value
S5 A	KEGG_CELL_CYCLE	-1.823	<0.0001
S5 B	GO_REGULATION_OF_CELL_DIVISION	-1.885	<0.0001
S5 C	REACTOME_CELL_CYCLE	-1.825	<0.0001
S5 D	GO_CELL_DIVISION	-1.899	<0.0001
S5 E	HALLMARK_APOPTOSIS	1.891	<0.0001
S5 F	HALLMARK_P53_PATHWAY	1.744	<0.0001
S6B	GO_MYELOID_CELL_DIFFERENTIATION	1.820	<0.0001
S6 C	GO_POSITIVE_REGULATION_OF_LYMPHOCYTE_ DIFFERENTIATION	1.721	<0.0001

Supplementary Table S5. Table showing gene ontology gene sets from gene set enrichment analysis in MLL-AF9/Mn1wt and MLL-AF9/Mn1null cells (see excel file).

Supplementary Table S6. Top 50 differentially expressed genes in MLL-AF9/Mn1wt versus MLL-AF9/Mn1null cells (see excel file).

Supplementary Table S7. Top 50 differentially expressed Hoxa9/a10 target genes between arrays for MLL-AF9/Mn1wt and MLL-AF9/Mn1null cells (see excel file).

References:

1. Sharma A, Yun H, Jyotsana N, Chaturvedi A, Schwarzer A, Yung E, et al. Constitutive IRF8 expression inhibits AML by activation of repressed immune response signaling. Leukemia. 2015 Jan;29(1):157-68.
2. Heuser M, Sly LM, Argiropoulos B, Kuchenbauer F, Lai C, Weng A, et al. Modeling the functional heterogeneity of leukemia stem cells: role of STAT5 in leukemia stem cell self-renewal. Blood. 2009 Nov 5;114(19):3983-93.
3. Sharma A, Yun H, Jyotsana N, Chaturvedi A, Schwarzer A, Yung E, et al. Constitutive IRF8 expression inhibits AML by activation of repressed immune response signaling. Leukemia, 2014.
4. Heuser M, Yap DB, Leung M, de Algara TR, Tafech A, McKinney S, et al. Loss of MLL5 results in pleiotropic hematopoietic defects, reduced neutrophil immune function, and extreme sensitivity to DNA demethylation. Blood. 2009 Feb 12;113(7):1432-43.
5. Sharma A, Jyotsana N, Lai CK, Chaturvedi A, Gabdoulline R, Gorlich K, et al. Pyrimethamine as a Potent and Selective Inhibitor of Acute Myeloid Leukemia Identified by High-throughput Drug Screening. Curr Cancer Drug Targets. 2016;16(9):818-28.
6. Jyotsana N, Sharma A, Chaturvedi A, Scherr M, Kuchenbauer F, Sajti L, et al. RNA interference efficiently targets human leukemia driven by a fusion oncogene in vivo. Leukemia. 2018 Jan;32(1):224-6.
7. Gautier L, Cope L, Bolstad BM, Irizarry RA. affy--analysis of Affymetrix GeneChip data at the probe level. Bioinformatics. 2004 Feb 12;20(3):307-15.
8. Ritchie ME, Phipson B, Wu D, Hu Y, Law CW, Shi W, et al. limma powers differential expression analyses for RNA-sequencing and microarray studies. Nucleic Acids Res. 2015 Apr 20;43(7):e47.
9. Deshpande AJ, Deshpande A, Sinha AU, Chen L, Chang J, Cihan A, et al. AF10 regulates progressive H3K79 methylation and HOX gene expression in diverse AML subtypes. Cancer Cell. 2014 Dec 8;26(6):896-908.
10. Bernt KM, Zhu N, Sinha AU, Vempati S, Faber J, Krivtsov AV, et al. MLL-rearranged leukemia is dependent on aberrant H3K79 methylation by DOT1L. Cancer Cell. 2011 Jul 12;20(1):66-78.

11. Huang Y, Sitwala K, Bronstein J, Sanders D, Dandekar M, Collins C, et al. Identification and characterization of Hoxa9 binding sites in hematopoietic cells. Blood. 2012 Jan 12;119(2):388-98.

12. Heuser M, Yun H, Berg T, Yung E, Argiropoulos B, Kuchenbauer F, et al. Cell of origin in AML: susceptibility to MN1-induced transformation is regulated by the MEIS1/AbdB-like HOX protein complex. Cancer Cell. 2011 Jul 12;20(1):39-52.

13. Zhang Y, Liu T, Meyer CA, Eeckhoute J, Johnson DS, Bernstein BE, et al. Model-based analysis of ChIP-Seq (MACS). Genome Biol. 2008;9(9):R137.

14. Ambrosini G, Dreos R, Kumar S, Bucher P. The ChIP-Seq tools and web server: a resource for analyzing ChIP-seq and other types of genomic data. BMC Genomics. 2016 Nov 18;17(1):938.